Piezoelectric MEMS Acoustic Sensor Array for Wideband Acoustic Emission Sensing

Talha Masood Khan(✉), Mohammad Merei, and Didem Ozevin

College of Engineering, University of Illinois at Chicago, Chicago, IL 60607, USA
{tkhan41,dozevin}@uic.edu

Abstract. In this study, the design of an array of piezoelectric MEMS acoustic emission sensors are introduced. A piezoelectric multi-user MEMS process (Piezo-MUMPs) is used to microfabricate a 4 × 4 array diaphragms ranging from 100 kHz to 700 kHz on a 5 mm × 5 mm chip. The numerical models of sensor array are built to understand the responses of both individual elements and array. The sensitivities of these sensors are compared to demonstrate an improvement in the sensitivity of array configuration. These sensors can operate in air-coupled, solid-coupled and fluid-coupled applications for damage detection in solids. They can be used for detecting damage modes in materials by differentiating the frequency components at the sensor level. Low cost and mass fabrication of the developed sensor enables a dense distributed sensor network for cyber physical systems.

Keywords: Multi-frequency · MEMS · Acoustic emission · Wideband

1 Introduction

Acoustic Emission (AE) is a passive structural health monitoring method where propagating elastic waves released by active defects trigger AE sensor to convert displacement response into electrical signal. The AE method has been applied to a wide range of infrastructure systems such as bridges [1–3], railways [4, 5] and pipelines [6–8]. The selection of AE sensor for a specific application plays significant role as it is the interface between input and output signals. The main characteristics of AE sensors include frequency bandwidth, sensitivity, and size. AE source (e.g., fatigue crack, wire break), structure type (e.g., concrete, steel), target resolution (controlled by attenuation) and space limitation are factors to select the most suitable AE sensors. Conventional AE sensors are bulky piezoelectric sensors manufactured manually and their size controls their frequency bandwidth. In recent years, MEMS AE sensors have been developed and tested in laboratory scale experiments [9]. They are based on capacitive and piezoelectric transduction mechanisms. Capacitive MEMS AE sensors require DC power, which limits their use in the applications with low power needs. With new micromaching techniques, piezoelectric MEMS gained significant potential. In this paper, the first-generation piezoelectric MEMS AE sensors developed in our laboratory are presented. Their limitation of low sensitivity and narrow frequency bandwidth are addressed in next generation by connecting a range of individual sensors tuned to different frequencies in series.

P. Rizzo and A. Milazzo (Eds.): EWSHM 2022, LNCE 253, pp. 640–645, 2023.
https://doi.org/10.1007/978-3-031-07254-3_65

2 The First-Generation Piezoelectric MEMS AE Sensors

The first-generation piezoelectric MEMS AE sensors are manufactured using piezo MUMPs provided by MEMSCAP. It is a multi-layer process to build microstructures with aluminum nitride as piezoelectric element. The design can be divided into two parts: the flexible mechanical mass-spring system that oscillates when an acoustic signal is incident on it; the piezoelectric layer on the mechanical layer that converts the kinetic energy of the acoustic signal to a change in electricity. The piezoelectric layer, AlN, is sandwiched between the device Si layer and metal electrode. A cross-section and top view of the PMUT is show in Fig. 1. These structure each contain four edge-clamped beams whose mass and stiffness can be tuned to the required resonant frequency.

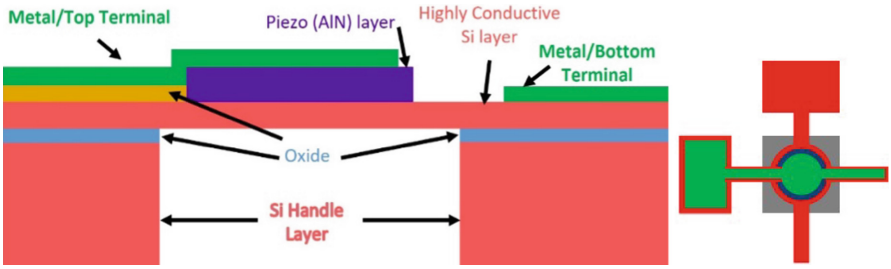

Fig. 1. (Left) Cross-sectional view of Piezo-MUMPs based pMUTs, (Right) Top view of a single pMUT sensor design. The central mass is suspended using 4 equidistance beams making an edge clamped beam-mass systems.

In the first-generation design, two sensors tuned to two frequencies were manufactured on a 4 mm × 4 mm die. The fundamental frequency of PMUT in the z-direction is proportional to $\sqrt{k/m}$, where k is the modal stiffness and m is the mass of the idealized suspended structure [10] as shown in Fig. 2. The factors controlling the fundamental frequency are cantilever lengths and width and diaphragm diameter. Thickness is controlled by micromachining process. The MEMS resonator has very high-quality factor leading to a narrow bandwidth frequency response. This is an advantage for dispersive medium with frequency dependent wave velocity. However, this is a disadvantage if the frequency of AE source is outside the AE sensor bandwidth.

Figure 3 shows the comparison of piezo MEMS and conventional AE sensors. As piezo MEMS are currently packaged with off-the-shelf ceramic package, the signal to noise ratio is low due to cabling. On the other hand, when amplitude/size ratios of two sensors are compared, shown in Fig. 3c, piezo MEMS have superior behavior as 99.59 as compared to conventional AE sensor as 1.24.

The results of the first-generation MEMS sensor indicate the promising performance as AE sensor that is a candidate to replace bulky sensors if bandwidth and signal to noise ratio are increased. In the second-generation design, bandwidth and sensitivity are tackled by connecting multiple frequency sensors in series as described below.

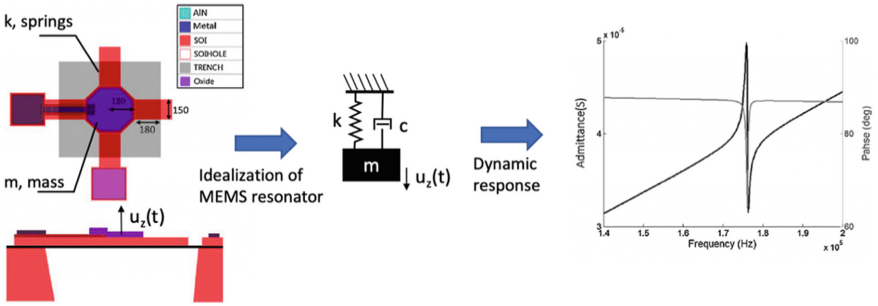

Fig. 2. The first-generation MEMS AE sensor operating as MEMS resonator near 175 kHz frequency.

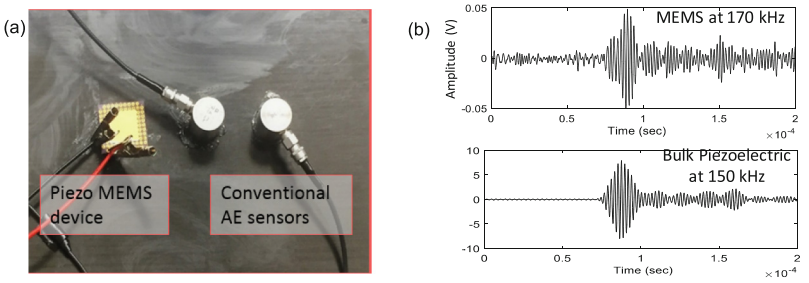

(c)

Sensor	Diameter/Width (mm)	Thickness (mm)	Total Size (mm^3)	Maximum Signal Amplitude (V)	Amplitude/Size (mV/mm^3)
MEMS at 170 kHz	0.7	1	0.49	0.048	99.59
Bulk Piezoelectric at 150 kHz	19.05	22.35	6373	7.939	1.24

Fig. 3. Comparison of piezo MEMS AE sensor with conventional AE sensors, (a) sensors coupled to composite layer, (b) time history signals and (c) comparison in amplitude to size.

3 The Second-Generation Piezoelectric MEMS AE Sensors

The second-generation design is aimed to include sixteen resonators tuned in the range of 100 kHz to 700 kHz with 40 kHz step. The design variables to tune the fundamental frequency are length and width of cantilever arms and mass of suspended diaphragm. Following the material properties of the design layers provided by the design rule limitations of PiezoMUMPs, each resonator is numerically modeled using COMSOL Multiphysics software with two physics modules namely solid mechanics and electrostatics module. Material properties used for Si and AlN layers for density (ρ (kg m^{-3})) are 2330 and 3300, Young's Modulus (E (GPa)) are 156 and 320, while the Poisson's ratio (ν) is 0.125 and 0.24 respectively, respectively [11–13]. In order to keep the area of piezoelectric layer constant, the diameter of octagonal central mass is selected the same for all the resonators as 300 μm. The width of beams is set the same as 125 μm for all the designs. The length of beams is the main variable to tune each resonator's frequency. It is varied

from 340 μm to 55 μm for the lowest and the highest frequency designs. Figure 4 shows the mode shapes of 100 kHz and 700 kHz designs. Entire diaphragm of 100 kHz design is under the same strain which is expected to produce higher current. The higher frequency design has varying strain distribution along piezoelectric layer, which requires the integration of strain distribution along diaphragm to convert displacement response into current.

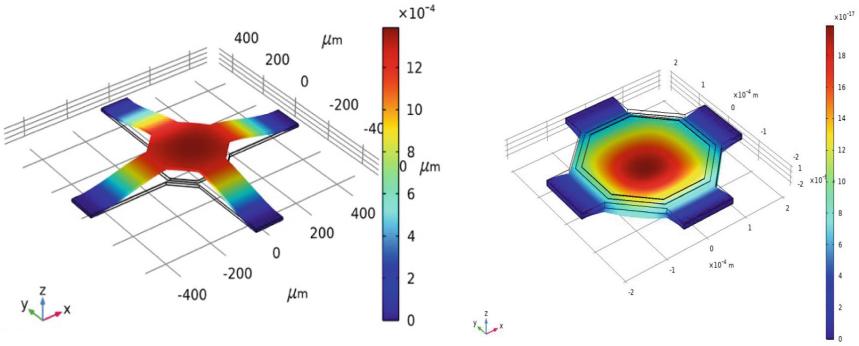

Fig. 4. The fundamental mode shapes of 100 kHz (left) and 700 kHz (right) MEMS AE sensors.

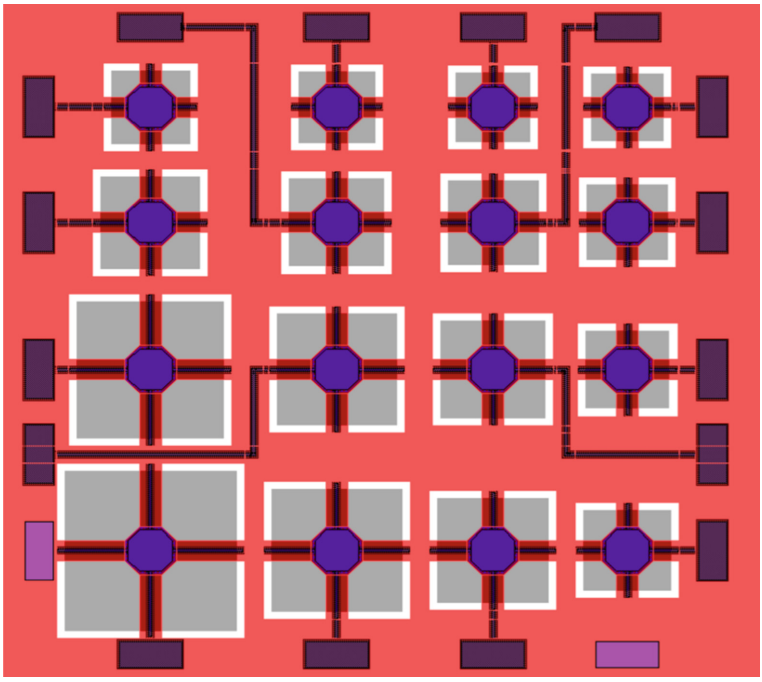

Fig. 5. LEdit design of 16 MEMS resonators on a 5 mm × 5 mm die space.

Each individual frequency sensor is simulated to ensure that their higher order modes do not coincide with the other frequencies in the array leading to destructive interference and the cancellation of signals in the summation. The array elements are then arranged so that they can work individually as well as an array as shown in Fig. 5.

4 Fabrication Process

The MEMS AE sensors are microfabricated by using a piezo-MultiUser MEMS processes (PiezoMUMPs) by MEMSCAP [11]. This is a 5-mask level Silicon on Insulator (SOI) patterning and etching process derived from work performed at MEMSCAP. The first layer is the piezoelectric layer, PZFILM, which is 0.5 microns of Aluminum Nitride (AlN). The second layer is the Pad Metal which is the metal stack of 20 nm of chrome and 1 μm if aluminum is patterned through a liftoff process. The fabrication process starts by using silicon on SOI wafer as substrate with Silicon thickness 10 ± 1 μm, Oxide thickness 1 ± 0.05 μm, and Handle wafer (Substrate) thickness of 400 ± 5 μm. The silicon layer is then doped by depositing the phosphosilicate glass layer (PSG) and annealed at 1050 °C for 1 h in Argon which removes the PSG via wet chemical etching. Then the wafer is coated with a positive photoresist and lithographically patterned by exposing the photoresist with light through the first level mask defined as PADOXIDE which remains after etching a reactive ion etch (RIE). Then Deep reactive ion etching (DRIE) is used to etch the silicon later down to the oxide layer. After this DRIE, the photoresist is chemically stripped. Then to ensure that wafer hold together through trench etching, we applied a polyimide coat onto the top surface of the patterned silicon layer. The bottom side of the wafers is coated with photoresist and the fifth level (TRENCH) is lithographically patterned. Then the Reactive ion (RIE) is used to remove the Bottom Side Oxide Layer and DRIE is used to remove the photoresist. A wet oxide etch process is then used to remove the Buried Oxide layer in the regions defined by the TRENCH mask. Lastly, the front side protection material is then stripped in a dry etch process. This releases any mechanical structures in the Silicon layer that are located over through-holes defined in the Substrate layer (Fig. 1). Following this process, the dies will be post processed using a process that involves bonding them to a wafer carrier and wire bonded for external connections.

As the microfabrication processes are not perfect [14], once the sensors are fabricated, they will be measured optically to measure the differences in lateral or vertical dimensions. The change in dimensions can be simulated again to identify variations in the design frequencies. We will the measure the impedance of the microfabricated sensors in both single element and array configurations. These results will then be compared to the updated simulation results to verify the designs. These sensors will then be tested in conjunction with ultrasonic transmitters on steel and composite materials under various experimental conditions.

5 Conclusions

This study is directed towards the design of MEMS Acoustic Emission sensor array with the improved sensitivity and frequency bandwidth. An array of sixteen piezoelectric resonators tuned in the range of 100 kHz to 700 kHz is designed to be operated as

individual sensors or single sensor to detect elastic waves within this frequency range. Each frequency is selected to ensure that their higher modes do not coincide with frequencies of other sensors such that they operate as constructive interference when they are connected in series. The sensors are currently being microfabricated by MEMSCAP.

Acknowledgment. This research was funded by National Science Foundation under Award No. IIP 2016444 entitled "PFI-TT: Multi-Frequency Acoustic Device for Rapid Infrastructure Damage Diagnostics". The support from the sponsoring organization is gratefully acknowledged. Any opinions, findings, and conclusions or recommendations expressed in this material are those of the authors and do not necessarily reflect the views of the sponsoring organization.

References

1. Nair, A., Cai, C.S.: Acoustic emission monitoring of bridges: review and case studies. Eng. Struct. **32**, 1704–1714 (2010)
2. Anay, R., Lane, A., Jauregui, D.V., Weldon, B.D., Soltangharaei, V., Ziehl, P.: On-site acoustic-emission monitoring for a prestressed concrete BT-54 AASHTO girder bridge. ASCE J. Perform. Constr. Facil. **34**(3), 04020034 (2020)
3. Megid, W.A., Chainey, M.A., Lebrun, P., Hay, R.: Monitoring fatigue cracks on eyebards of steel bridges using acoustic emission: a case study. Eng. Fract. Mech. **211**, 198–208 (2019)
4. Janeliukstis, R., Clark, A., Papaelias, M., Kaewunruen, S.: Flexural cracking-induced acoustic emission peak frequency shift in railway prestressed concrete sleepers. Eng. Struct. **178**, 493–505 (2019)
5. Carboni, M., Crivelli, D.: An acoustic emission based structural health monitoring approach to damage development in solid railway axles. Int. J. Fatigue **139** (2020)
6. Baran, I., Lyasota, I., Skrok, K.: Acoustic emission testing of underground pipelines of crude oil of fuel storage depots. J. Acoust. Emiss. **33**, S9 (2016)
7. Smith, A., et al.: Acoustic emission sensing of pipe–soil interaction: full-scale pipelines subjected to differential ground movements. J. Geotech. Geoenviron. Eng. **145**(12), 4019113 (2019)
8. Quy, T.B., Kim, J.-M.: Crack detection and localization in a fluid pipeline based on acoustic emission signals. Mech. Syst. Sig. Process. **150**, 107254 (2021)
9. Ozevin, D.: MEMS acoustic emission sensors. Appl. Sci. **10**, 8966 (2020)
10. Kabir, M., Kazari, H., Ozevin, D.: Piezoelectric MEMS acoustic emission sensors. Sens. Actuators A **279**, 53–64 (2018)
11. Cowen, A., Hames, G., Glukh, K., Hardy, B.: PiezoMUMPs Design Handbook, Revision 1.3 edn. MEMSCAP Inc. (2014)
12. Setter, N., et al.: Ferroelectric thin films: review of materials, properties, and applications. J. Appl. Phys. **100**(5), 051606 (2006)
13. Dubois, M.-A., Muralt, P.: Properties of aluminum nitride thin films for piezoelectric transducers and microwave filter applications. Appl. Phys. Lett. **74**(20), 3032–3034 (1999)
14. Baborowski, J.: Microfabrication of Piezoelectric MEMS. In: Setter, N. (eds.) Electroceramic-Based MEMS. EMST, vol. 9, pp. 325-359. Springer, Boston (2005). https://doi.org/10.1007/0-387-23319-9_13